JOURNAL OF AIRCRAFT
Vol. 47, No. 5, September–October 2010

Data Mining of Pareto-Optimal Transonic Airfoil Shapes Using Proper Orthogonal Decomposition

Akira Oyama*
Japan Aerospace Exploration Agency, Sagamihara 229-8510, Japan
Taku Nonomura†
University of Tokyo, Sagamihara 229-8510, Japan
and
Kozo Fujii‡
Japan Aerospace Exploration Agency, Sagamihara 229-8510, Japan

DOI: 10.2514/1.C000264

A new approach to extract useful design information from the shape data of Pareto-optimal solutions of an optimization problem is proposed and applied to the optimization of airfoil shapes for good aerodynamic performance at transonic speed. The proposed approach decomposes shape data into principal modes and corresponding base vectors, using proper orthogonal decomposition. The advantage of the proposed approach is that the knowledge one can obtain does not depend on how the shape is parameterized for design optimization. Analysis of the airfoil shapes obtained as the Pareto-optimal solutions for aerodynamic performance at transonic speeds shows that the optimized airfoils can be categorized into three families (low-drag designs, high-lift-to-drag designs, and high-lift designs), where the lift is increased by changing the camber near the trailing edge among the low-drag designs, while the lift is increased by moving the lower surface upward among the high-lift designs.

Nomenclature

$a_m(n)$	=	eigenvector of mode m
C_d	=	drag coefficient
C_l	=	lift coefficient
c	=	chord length
j	=	index of grid points
j max	=	number of grid points
m	=	index of modes
m max	=	number of modes
n	=	index of Pareto-optimal solutions
n max	=	number of Pareto-optimal solutions
$S_{m1,m2}$	=	covariance of y'_{base} of mode $m1$ and mode $m2$
$x(j,n)$	=	coordinate in chordwise direction
$y(j,n)$	=	coordinate in normal direction of the Pareto-optimal solution n at grid point j
$y_{l/d_{\text{ave}}}(j)$	=	y coordinate of maximum lift-to-drag-ratio design at grid point j
$y'(j,n)$	=	fluctuation of y coordinate of Pareto-optimal solution n at grid point j
$y'_{\text{base}}(j,m)$	=	orthogonal base vector of mode m

I. Introduction

MULTIOBJECTIVE design exploration [1] (MODE) is a framework to extract essential knowledge of a multiobjective design optimization problem, such as tradeoff information between contradicting objectives and the effect of each design parameter on the objectives. In the framework of MODE, Pareto-optimal solutions are obtained by multiobjective optimization, using (for example) a multiobjective evolutionary algorithm [2], and then important design knowledge is extracted by analyzing the values of objective functions and design parameters of the obtained Pareto-optimal solutions. There, data-mining approaches, such as the self-organizing map [3] and analysis of variance [4], are used. Recently, MODE framework has been applied to a wide variety of design optimization problems, including multidisciplinary design of a regional-jet wing [5,6], aerodynamic design of the flyback booster of a reusable launch vehicle [7], aerodynamic design of a flapping airfoil [8], and aerodynamic design of a turbine blade for a rocket engine [9].

Although data-mining approaches of the values of objective functions and design parameters are useful, still better approaches would be required. Design knowledge of the shape design optimization problem one can obtain depends on how the shape is parameterized. For example, if an airfoil shape is represented by *B*-spline curves and the coordinates are considered as the design parameters, it is difficult to obtain design knowledge related to leading-edge radius, thickness distribution, and so on. To date, there is no efficient approach for the analysis of shape data, as far as the authors know.

Proper orthogonal decomposition (POD, known as the Karhunen–Loeve expansion in pattern recognition and principal component analysis in the statistical literature) is a statistical approach that can extract dominant features in data by decomposing the data into a set of optimal orthogonal base vectors of decreasing importance. These base vectors are optimal, in the sense that any other set of orthogonal base vectors cannot capture more information than the orthogonal base vectors obtained by POD as long as the number of base vectors is limited. The POD has been used to analyze unsteady flow data, such as the vorticity fields of a flow in a flume [10] and jet/vortex interaction [11]. It has also been extensively used in image processing (for example, see [12]), structural vibration analysis, and so on.

In the last decade, POD has also been used for design optimization [13–18]. In [13,14], POD is used to reduce the computational cost required to solve the Euler equations. In [15,16], POD is used to recognize the most contradicting objective functions and to reduce the number of objective functions in various problems. References [17,18] propose to use POD to reduce the number of design

Presented as Paper 2009-4000 at the 19th AIAA Computational Fluid Dynamics, San Antonio, TX, 22–25 June 2009; received 18 January 2010; revision received 25 March 2010; accepted for publication 25 March 2010.

*Assistant Professor, Institute of Space and Astronautical Science, Department of Space Transportation Engineering, 3-1-1 Yoshinodai. Member AIAA.

†Research Associate, Department of Aeronautics and Astronautics, 3-1-1 Yoshinodai. Member AIAA.

‡Professor, Department of Space Transportation Engineering, Institute of Space and Astronautical Science, 3-1-1 Yoshinodai. Fellow AIAA.

parameters. In these references, POD is applied to the values of the user-defined design parameters of optimized designs, and then the optimization is continued with the obtained eigenvectors of principal modes as new design parameters. The motivation of all the former research listed previously is improvement of the optimization process.

The objective of the present study is to propose a new approach that extracts useful design information from the shape data of Pareto-optimal solutions of optimization problems and to apply this approach to aerodynamic transonic airfoil shape optimization data to extract knowledge related to aerodynamic transonic airfoil design. The proposed approach enables analysis of the shape data of all Pareto-optimal solutions by decomposing the shape data into principal modes and eigenvectors, using POD. To show the capability of the proposed approach, information obtained with POD is compared with that obtained with the traditional approach (analysis of design parameters).

II. Pareto-Optimal Solutions

The Pareto-optimal solutions of the design optimization problem are considered. The objective functions are lift coefficient (maximization) and drag coefficient (minimization). The constraints are that the lift coefficient must be greater than zero, and the maximum thickness must be greater than a 0.10 chord length. The design parameters are coordinates of six control points of the *B*-spline curves representing an airfoil shape (Fig. 1). The flow conditions are a freestream Mach number of 0.8, a Reynolds number of 10^6 (based on the chord length), and an angle of attack of 2 deg.

The Pareto-optimal solutions are obtained by a multiobjective evolutionary algorithm (MOEA), used in [8]. The present MOEA adopts real-number coding, which enables efficient search in real-number optimizations when compared with binary or gray coding. The population size is maintained at 64, and the maximum number of generations is set to 60. The initial population is generated randomly, so that the initial population covers the entire design space presented in Table 1. The fitness of each design candidate is computed according to Pareto-ranking, fitness sharing, and Pareto-based constraint handling [19], based on its objective function and constraint function values. Here, Fonseca and Fleming's Pareto-based ranking method [20] and the fitness sharing method of Goldberg and Richardson [21] are used for Pareto-ranking, where each individual is assigned a rank according to the number of individuals dominating it. In Pareto-based constraint handling, the rank of feasible designs is determined by the Pareto-ranking based on the objective function values, whereas the rank of infeasible designs is determined by the Pareto-ranking based on the constraint function values. The parents of the new generation are selected through roulette selection [22] from the best 64 individuals among the present generation and the best 64 individuals in the previous generation. A new generation is reproduced through crossover and mutation operators. The term crossover refers to an operator that combines the genotype of the selected parents and produces new individuals, with the intent of improving the fitness value of the next generation. Here, the blended crossover [23], where the value of α is 0.5, is used for crossover between the selected solutions. Mutation is applied to the design parameters of the new generation to maintain diversity. Here, the probability of mutation taking place is 20%; this adds a random disturbance to the corresponding gene of up to 10% of the given range of each design parameter. Present MOEA to find quasi-optimal solutions has been well validated [24,25].

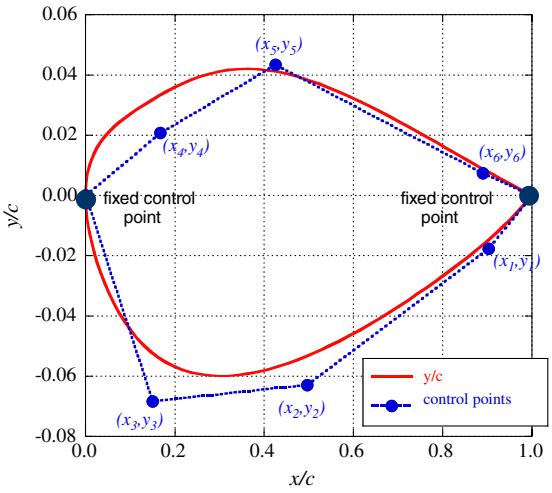

Fig. 1 Parameterization of the airfoil shape. The coordinates of six control points of the *B*-spline curves, representing an airfoil shape, are considered as design parameters.

Table 1 Search range of each design parameter

Design parameter	Lower bound	Upper bound
x_1	0.66	0.99
x_2	0.33	0.66
x_3	0.01	0.33
x_4	0.01	0.33
x_5	0.33	0.66
x_6	0.66	0.99
y_1	−0.10	0.10
y_2	−0.10	0.10
y_3	−0.10	0.10
y_4	0.00	0.20
y_5	0.00	0.20
y_6	0.00	0.20

Lift and drag coefficients of each design candidate are evaluated, using a two-dimensional Reynolds-averaged Navier–Stokes solver. This code employs total-variation-diminishing-type upwind differencing [26], the lower–upper symmetric Gauss–Seidel scheme [27], the turbulence model of Baldwin and Lomax [28], and the multigrid method [29] for the steady-state problems.

All the design candidates and Pareto-optimal solutions are plotted in Fig. 2. The number of Pareto-optimal solutions obtained is 85. A strong tradeoff between lift maximization and drag minimization is observed. This figure also indicates that there are two groups in the obtained Pareto-optimal solutions: low-drag design group (roughly, $C_l < 0.75$) and high-lift design group (roughly, $C_l > 0.75$). The maximum-lift, maximum lift-to-drag ratio, and minimum-drag airfoil shapes and corresponding static pressure distributions, shown in Fig. 3, indicate that the maximum-lift-to-drag-ratio and minimum-drag designs avoid generation of strong shock waves, while the maximum-lift design generates a large negative pressure region terminated with a shock wave. This figure also shows that the maximum lift-to-drag-ratio design has a shape that is similar to supercritical airfoils.

III. Data Mining of Shape Data of Pareto-Optimal Solutions Using Proper Orthogonal Decomposition

In this study, the airfoil shapes of the Pareto-optimal solutions are analyzed using the snapshot POD proposed by Sirovich [30]. The Pareto-optimal solutions from the minimum-drag design to the maximum-lift design are numbered, as shown in Fig. 4. The shape data to be analyzed here are y coordinates on all the grid points around the airfoil, as shown in Fig. 5. The number of grid points around an airfoil are 137.

In the original snapshot POD, the data to be analyzed are decomposed into the mean vector and the fluctuation vector, which are defined from the mean vector. It is known that analysis of the fluctuation from the mean vector maximizes variance of the data. However, for analysis of Pareto-optimal solutions, it would be reasonable to define the fluctuation from one representative design (for example, the median design). Here, the fluctuation from the l/d-maximum design is analyzed. The shape data of the Pareto-optimal solutions are decomposed into the data of the maximum lift-to-drag-ratio design and fluctuation data as follows:

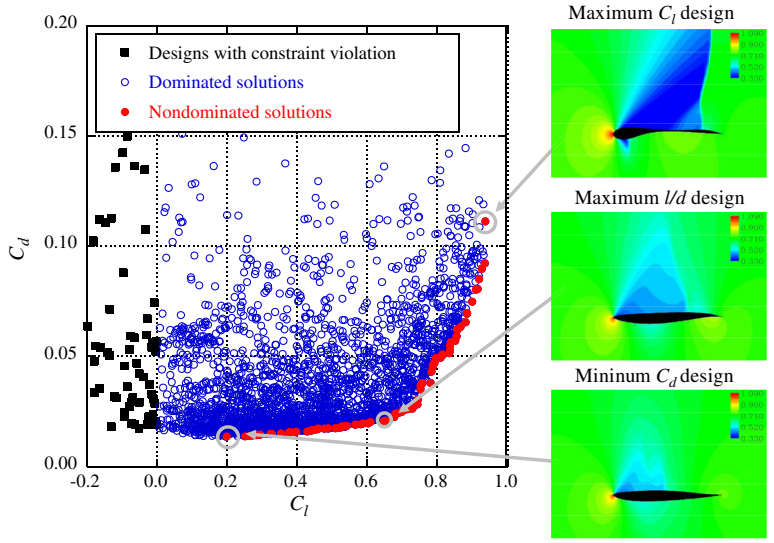

Fig. 2 Distribution of the Pareto-optimal solutions and other design candidates, with the pressure distribution around the minimum-drag, maximum lift-to-drag ratio, and maximum-lift airfoils.

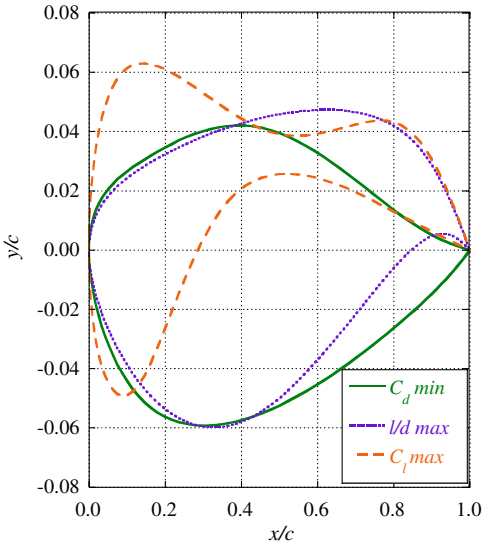

a) Airfoil shapes

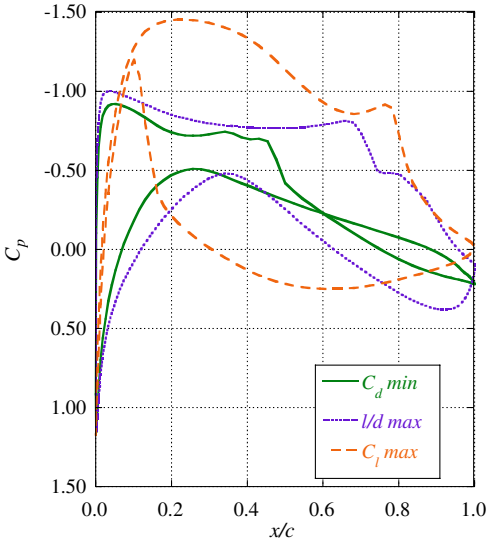

b) Surface pressure distributions

Fig. 3 Shape and surface pressure distributions of the minimum-drag, maximum lift-to-drag ratio, and maximum-lift airfoils.

$$\begin{bmatrix} y(1,n) \\ y(2,n) \\ \vdots \\ y(j\max-1,n) \\ y(j\max,n) \end{bmatrix} = \begin{bmatrix} y_{l/d_{\max}}(1) \\ y_{l/d_{\max}}(2) \\ \vdots \\ y_{l/d_{\max}}(j\max-1) \\ y_{l/d_{\max}}(j\max) \end{bmatrix} + \begin{bmatrix} y'(1,n) \\ y'(2,n) \\ \vdots \\ y'(j\max-1,n) \\ y'(j\max,n) \end{bmatrix} \tag{1}$$

The fluctuation vector is then expressed by the linear sum of the normalized eigenvectors and orthogonal base vectors as follows:

$$\begin{bmatrix} y'(1,n) \\ y'(2,n) \\ \vdots \\ y'(j\max-1,n) \\ y'(j\max,n) \end{bmatrix} = a_1(n) \begin{bmatrix} y'_{\text{base}}(1,1) \\ y'_{\text{base}}(2,1) \\ \vdots \\ y'_{\text{base}}(j\max-1,1) \\ y'_{\text{base}}(j\max,1) \end{bmatrix} + \cdots + a_{m\max}(n) \begin{bmatrix} y'_{\text{base}}(1,m\max) \\ y'_{\text{base}}(2,m\max) \\ \vdots \\ y'_{\text{base}}(j\max-1,m\max) \\ y'_{\text{base}}(j\max,m\max) \end{bmatrix} \tag{2}$$

where each eigenvector is determined, so that the energy defined by Eq. (3) is maximized as follows:

$$\sum_{j=1}^{j\max} y'^2_{\text{base}}(j,m), \qquad m = 1,2,\ldots,m\max \tag{3}$$

The eigenvectors that maximize the energy defined by Eq. (3) can be obtained by solving the eigenvalue problem of the following covariance matrix:

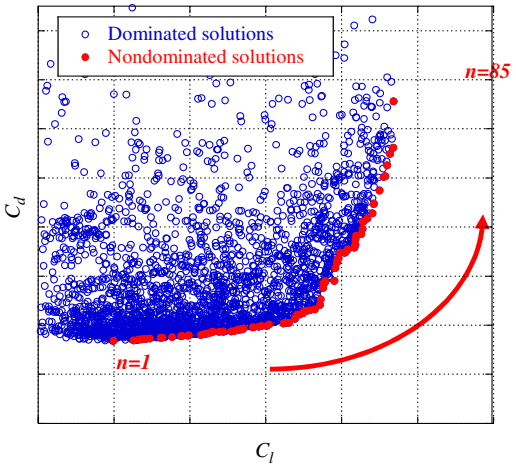

Fig. 4 Index of the Pareto-optimal solutions. For the minimum-drag design, $n = 1$, and for the maximum-lift design, $n = n\max = 85$.

$$\begin{pmatrix} S_{1,1} & \cdots & S_{m1,1} & \cdots & S_{m\max,1} \\ \vdots & \ddots & \vdots & & \vdots \\ S_{1,m2} & \cdots & S_{m1,m2} & \cdots & S_{m\max,m2} \\ \vdots & & \vdots & \ddots & \vdots \\ S_{1,m\max} & \cdots & S_{m1,m\max} & \cdots & S_{m\max,m\max} \end{pmatrix} \tag{4}$$

where

$$S_{m1,m2} = \sum_{j=1}^{j\max} y'(j,m1)y'(j,m2) \tag{5}$$

IV. Results

The shape data analyzed here are the y coordinates defined on all the grid points on the airfoil shape. The energy ratios of 10 principal orthogonal base vectors (principal POD modes) to the total energy are shown in Fig. 6. While the fluctuation from the airfoil shape data of the l/d maximum design is analyzed, principal modes are successfully extracted. The first mode is dominant (more than 83%) and the first two modes represent more than 94% of the total energy.

Figure 7 shows the components of the eigenvectors of the second modes, with respect to the index of the nondominated solutions n (left) and the lift coefficient $C_l(n)$ (right). Obtained nondominated airfoil shapes are categorized into three groups: the low-drag design group (roughly, $1 \le n \le 39$ and $C_l < 0.65$), the high-l/d design

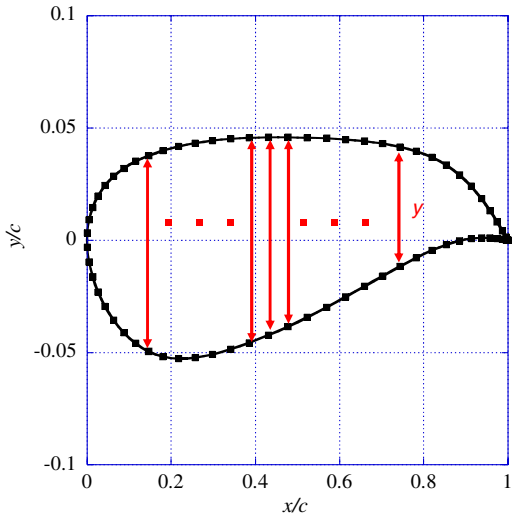

Fig. 5 Definition of the shape data. Shape data analyzed here are y coordinates defined on all grid points of the airfoil shape.

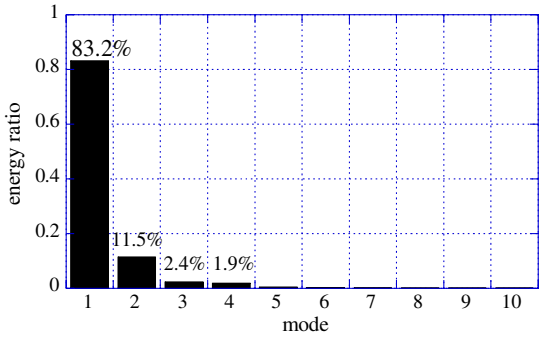

Fig. 6 Energy ratio of the top ten principal modes of the airfoil shape.

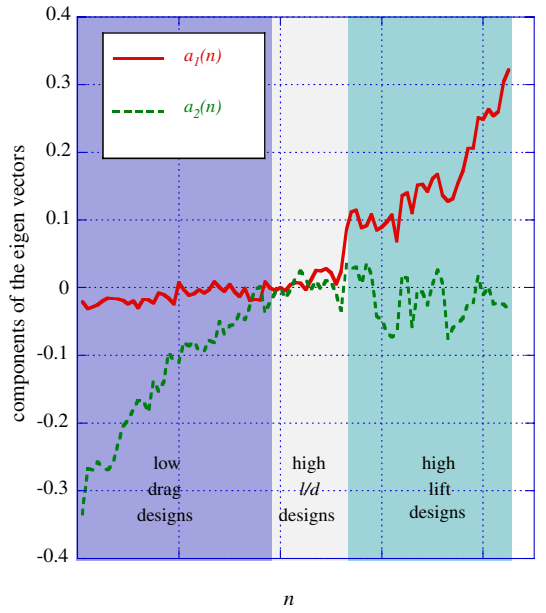

a) Components of the eigenvectors with respect to n

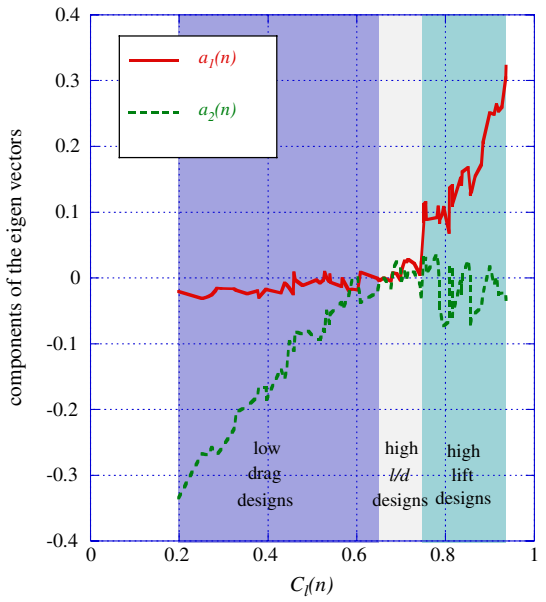

b) Components of the eigenvectors with respect to $C_l(n)$

Fig. 7 Components of the eigenvectors of the first and second modes.

group ($40 \leq n \leq 52$ and $0.65 < C_l < 0.75$), and the high-lift design group ($53 \leq n \leq 85$ and $C_l > 0.75$). As for the low-drag design group, the second mode is dominant, and the eigenvector of the first mode is approximately zero. Among the high-lift design group, the first mode is dominant, and the eigenvector of the second mode is small. The Pareto-optimal solutions in the high-l/d design group have no significant difference in the shape. A large jump in the first mode is observed between $n = 52$ and $n = 53$. This jump indicates a significant change in the shape between the high-l/d designs and the high-lift designs. Figure 8 compares shape and surface pressure distributions of the Pareto-optimal solutions ($n = 52$ and $n = 53$). This figure shows that there is a significant difference in the position of the shock wave due to the change in the airfoil shape itself. The Pareto-optimal solutions in the high-lift design group have a shock wave in the more aft part of the airfoil.

Figure 9 presents the l/d-maximum airfoil shape and the orthogonal base vectors of the first and second modes. This figure indicates that mode 1 changes the lower surface from the leading edge to the trailing edge. The base vector of mode 1 also indicates that thickness near the leading edge should be increased as the camber is increased. This comes from the constraint on the maximum thickness imposed on the design optimization problem. The base vector of the second mode indicates that the second mode mainly contributes to the camber near the trailing edge. The base vectors of modes 3 and 4 mainly contribute to the airfoil thickness near the trailing edge and the leading edge, respectively.

Recalling that the shapes of the Pareto-optimal solutions are represented by Eqs. (1) and (2), Figs. 7 and 9 indicate that the low-drag design group increases lift by changing the camber near the trailing edge, while the other part of the airfoil shape is almost fixed. As for the high-lift design group, lift is increased by moving the lower surface upward without significant change in the trailing-edge angle. This movement of the lower surface corresponds to the camber increase. The thickness near the leading edge is increased as the

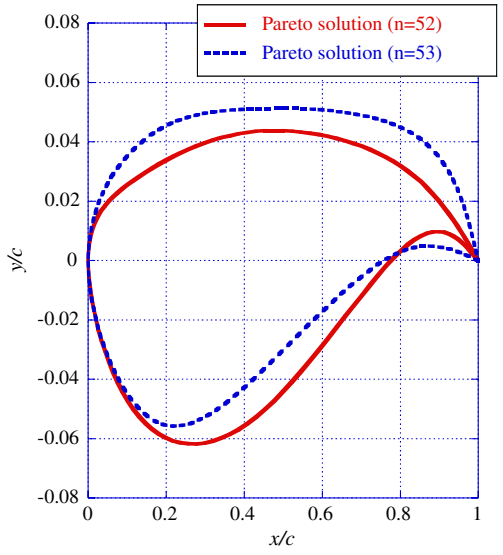

a) Airfoil shapes

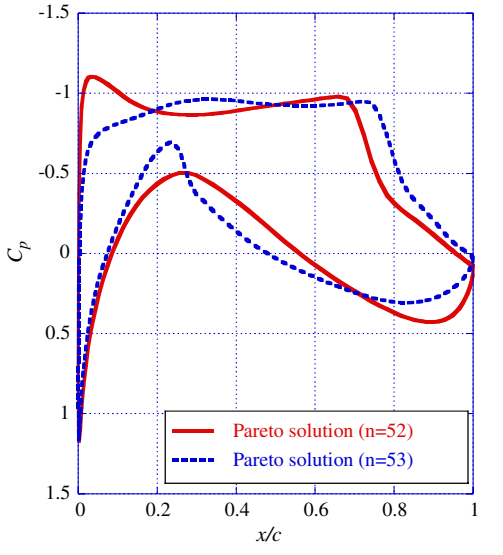

b) Surface pressure distributions

Fig. 8 Shape and surface pressure distributions of the Pareto-optimal solutions.

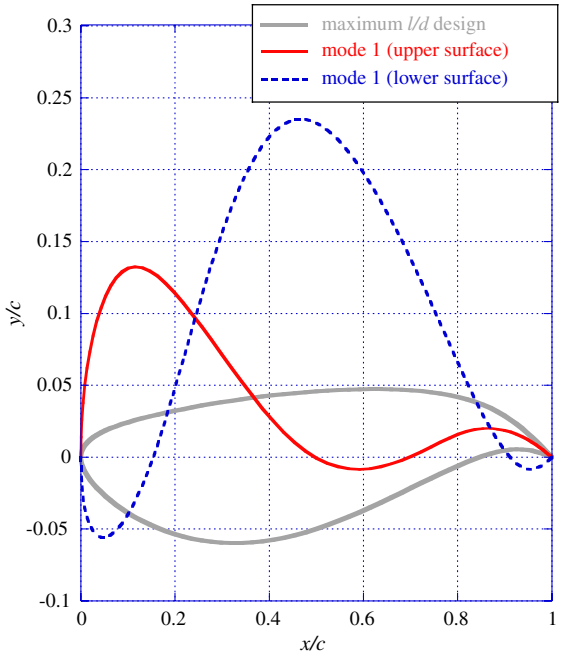

a) Base vector of the first mode

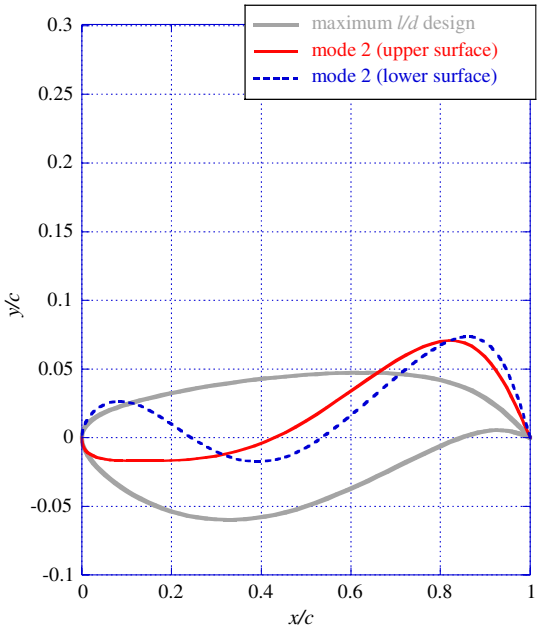

b) Base vector of the second mode

Fig. 9 Shape of the maximum lift-to-drag-ratio airfoil design and the orthogonal base vectors of the first and second modes.

lower surface moves upward to satisfy the constraint applied to the airfoil maximum thickness near the leading edge.

V. Comparison with Conventional Approach

To identify the advantage of the proposed approach over the conventional approach, design parameters of the Pareto-optimal designs are analyzed. Figure 10 presents scatter plots of the design parameters of the Pareto-optimal solutions against the lift coefficient (upper) and the drag coefficient (lower). These plots give us some of the following ideas:

1) The Pareto-optimal solutions may be categorized into two groups (see, for example, C_l against y_2 or y_4).

2) Airfoil camber increases as the lift increases.

However, analysis of this figure hardly leads to the design knowledge we obtained in the previous section, such as the following:

1) The Pareto-optimal solutions can be categorized into three groups.

2) Among the low-drag designs, lift is increased by changing the camber near the trailing edge.

3) Among the high-lift designs, the lift is increased by moving the lower surface upward. The reason for that is these features are represented by multiple design parameters. For example, the camber near the trailing edge is mainly represented by x_1, y_1, x_6, and y_6.

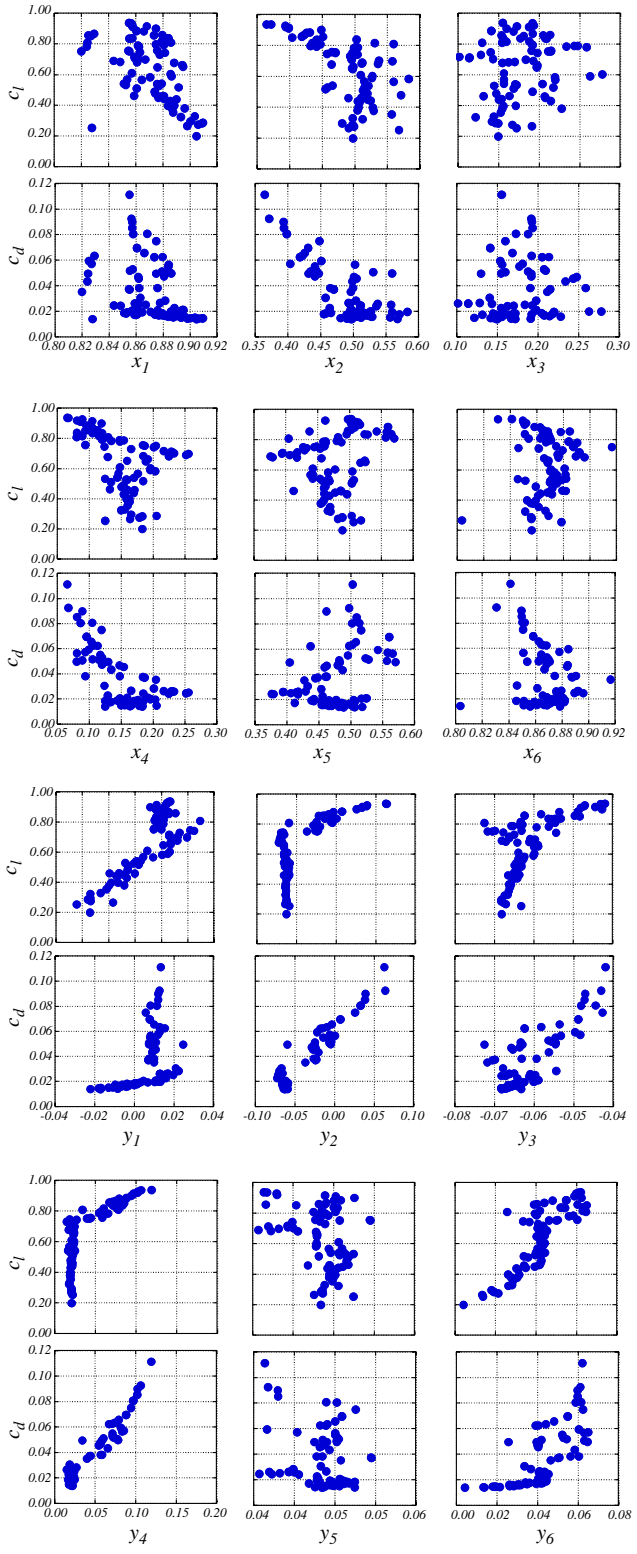

Fig. 10 Scatter plot matrix of the design parameters with respect to the lift or drag coefficients.

VI. Conclusions

A new approach to extract useful design information from the shape data of the Pareto-optimal solutions has been proposed and applied to an aerodynamic transonic airfoil shape optimization. The proposed approach decomposes the data of all Pareto-optimal solutions into principal modes and base vectors using POD. The advantage of the proposed approach is that the knowledge one can obtain does not depend on how the shape is parameterized for design optimization.

Data mining of the shape data of the Pareto-optimal solutions of an aerodynamic transonic airfoil shape optimization problem showed that the optimized airfoils can be categorized into three families: low-drag designs, high-lift-to-drag ratio designs, and high-lift designs. Among the low-drag designs, lift is increased by changing the camber near the trailing edge. Among the high-lift designs, the lift is increased by moving the lower surface upward, which corresponds to the increase in the camber.

Although the proposed method is applied to a two-objective optimization problem here, the proposed approach is also applicable to three or more objective optimization problems.

Acknowledgment

The present research was supported in part by the Japan Society for the Promotion of Science grants-in-aid for scientific research KAKENHI (20760552) and KAKENHI (20246122).

References

[1] Jeong, S., Chiba, K., and Obayashi, S., "Data Mining for Aerodynamic Design Space," *Journal of Aerospace Computing, Information, and Communication*, Vol. 2, No. 11, 2005, pp. 452–469. doi:10.2514/1.17308

[2] Deb, K., *Multiobjective Optimization Using Evolutionary Algorithms*, Wiley, Chichester, UK, 2001.

[3] Kohonen, T., *Self-Organizing Maps*, 2nd ed., Springer, Heidelberg, Germany, 1997.

[4] Donald, R. J., Matthias, S., and William, J. W., "Efficient Global Optimization of Expensive Black-Box Function," *Journal of Global Optimization*, Vol. 13, No. 4, 1998, pp. 455–492. doi:10.1023/A:1008306431147

[5] Chiba, K., Oyama, A., Obayashi, S., and Nakahashi, K., "Multidisciplinary Design Optimization and Data Mining for Transonic Regional-Jet Wing," *Journal of Aircraft*, Vol. 44, No. 4, 2007, pp. 1100–1112. doi:10.2514/1.17549

[6] Chiba, K., and Obayashi, S., "Data Mining for Multidisciplinary Design Space of Regional-Jet Wing," *Journal of Aerospace Computing, Information, and Communication*, Vol. 4, No. 11, 2007, pp. 1019–1036. doi:10.2514/1.19404

[7] Obayashi, S., and Chiba, K., "Knowledge Discovery for Flyback-Booster Aerodynamic Wing Using Data Mining," *Journal of Spacecraft and Rockets*, Vol. 45, No. 5, 2008, pp. 975–987. doi:10.2514/1.28511

[8] Oyama, A., Okabe, Y., Shimoyama, K., and Fujii, K., "Aerodynamic

Multiobjective Design Exploration of a Flapping Airfoil Using a Navier–Stokes Solver," *Journal of Aerospace Computing, Information, and Communication*, Vol. 6, No. 3, 2009, pp. 256–270. doi:10.2514/1.35992

[9] Tani, N., Oyama, A., and Yamanishi, N., "Multiobjective Design Optimization of Rocket Engine Turbopump Turbine," 5th International Spacecraft Propulsion Conference/2nd International Symposium on Propulsion for Space Transportation, Association Aéronautique et Astronautique de France Paper 154, Paris, 2008.

[10] Liberzon, A., Gurka, R., Tiselj, I., and Hetsroni, G., "Spatial Characterization of the Numerically Simulated Vorticity Fields of a Flow in a Flume," *Theoretical and Computational Fluid Dynamics*, Vol. 19, No. 2, 2005, pp. 115–125. doi:10.1007/s00162-004-0156-y

[11] Maurel, S., Boree, J., and Lumley, J. L., "Extended Proper Orthogonal Decomposition: Application to Jet/Vortex Interaction," *Flow, Turbulence and Combustion*, Vol. 67, No. 2, 2001, pp. 125–136. doi:10.1023/A:1014050204350

[12] Tabib, M. V., and Joshi, J. B., "Analysis of Dominant Flow Structures and Their Flow Dynamics in Chemical Process Equipment Using Snapshot Proper Orthogonal Decomposition Technique," *Chemical Engineering Science*, Vol. 63, No. 14, 2008, pp. 3695–3715. doi:10.1016/j.ces.2008.04.046

[13] LeGresley, P. A., and Alonso, J. J., "Airfoil Design Optimization Using Reduced Order Models Based on Proper Orthogonal Decomposition," AIAA Paper 2000-2545, June 2000.

[14] Goss, J., and Subbarao, K., "Inlet Shape Optimization Based on POD Model Reduction of the Euler Equations," AIAA Paper 2008-5809, Sept. 2008.

[15] Deb, K., and Saxena, D. K., "Searching For Pareto-Optimal Solutions Through Dimensionality Reduction for Certain Large-Dimensional Multiobjective Optimization Problems," *Proceedings of 2006 IEEE Congress on Evolutionary Computation*, IEEE Computer Society Press, Piscataway, NJ, 2006, pp. 3353–3360.

[16] Jeong, S., Lim, J. N., Obayashi, S., and Koishi, M., "Design Exploration into a Tire Noise Reduction Problem," International Workshop on Multidisciplinary Design Exploration in Okinawa 2006, Japan Society for Mechanical Engineers, 2006, pp. 77–82.

[17] Toal, D. J. J., Bressloff, N. W., and Keane, A. J., "Geometric Filtration Using POD for Aerodynamic Design Optimization," AIAA Paper 2008-6584, Aug. 2008.

[18] Li, G., Li, M., Azarm, S., Rambo, J., and Joshi, Y., "Optimizing Thermal Design of Data Center Cabinets with a New Multi-Objective Genetic Algorithm," *Distributed and Parallel Databases*, Vol. 21, Nos. 2–3, 2007, pp. 167–192. doi:10.1007/s10619-007-7009-9

[19] Oyama, A., Shimoyama, K., and Fujii, K., "New Constraint-Handling Method for Multi-Objective Multi-Constraint Evolutionary Optimization," *Transactions of the Japan Society for Aeronautical and Space Sciences*, Vol. 50, No. 167, 2007, pp. 56–62. doi:10.2322/tjsass.50.56

[20] Fonseca, C. M., and Fleming, P. J., "Genetic Algorithms for Multiobjective Optimization: Formulation, Discussion and Generalization," *Proceedings of the 5th International Conference on Genetic Algorithms*, edited by S. Forrest, Morgan Kaufmann, San Mateo, CA, 1993, pp. 416–423.

[21] Goldberg, D. E., and Richardson, J., "Genetic Algorithms with Sharing for Multimodal Function Optimization," *Proceedings of the Second International Conference on Genetic Algorithms*, Lawrence Erlbaum Associates, Mahwah, NJ, 1987, pp. 41–49.

[22] Goldberg, D. E., *Genetic Algorithms in Search, Optimization and Machine Learning*, Addison Wesley Longman, Reading, MA, 1989.

[23] Eshelman, L. J., and Schaffer, J. D., "Real-Coded Genetic Algorithms and Interval Schemata," *Foundations of Genetic Algorithms 2*, edited by L. D. Whitley, Morgan Kaufmann, San Mateo, CA, 1993, pp. 187–202.

[24] Obayashi, S., Sasaki, D., and Oyama, A., "Finding Tradeoffs by Using Multiobjective Optimization Algorithms," *Transactions of the Japanese Society for Aeronautical and Space Sciences*, Vol. 47, No. 155, 2004, pp. 51–58. doi:10.2322/tjsass.47.51

[25] Oyama, A., and Liou, M. S., "Multiobjective Optimization of Rocket Engine Pumps Using Evolutionary Algorithm," *Journal of Propulsion and Power*, Vol. 18, No. 3, 2002, pp. 528–535. doi:10.2514/2.5993

[26] Obayashi, S., and Wada, Y., "Practical Formulation of a Positively Conservative Scheme," *AIAA Journal*, Vol. 32, No. 5, 1994, pp. 1093–1095. doi:10.2514/3.12104

[27] Obayashi, S., and Guruswamy, G. P., "Convergence Acceleration of an Aeroelastic Navier–Stokes Solver," *AIAA Journal*, Vol. 33, No. 6, 1995, pp. 1134–1141. doi:10.2514/3.12533

[28] Baldwin, B. S., and Lomax, H., "Thin-Layer Approximation and Algebraic Model for Separated Turbulent Flows," AIAA Paper 1978-0257, Jan. 1985.

[29] Brant, A., "Multi-Level Adaptive Solutions to Boundary Value Problems," *Mathematics of Computation*, Vol. 31, No. 138, 1977, pp. 333–390. doi:10.2307/2006422

[30] Sirovich, L., "Turbulence and Dynamics of Coherent Structures Part 1: Coherent Structures," *Quarterly of Applied Mathematics*, Vol. 45, No. 3, 1987, pp. 561–571.